Near-Threshold Production of ϕ Mesons in pp Collisions

M. Hartmann,[1,*] Y. Maeda,[1,2] I. Keshelashvili,[1,3] H. R. Koch,[1] S. Mikirtytchiants,[4] S. Barsov,[4] W. Borgs,[1] M. Büscher,[1] V. I. Dimitrov,[5] S. Dymov,[6] V. Hejny,[1] V. Kleber,[7] V. Koptev,[4] P. Kulessa,[1,8] T. Mersmann,[9] S. Merzliakov,[6] A. Mussgiller,[1] M. Nekipelov,[1] M. Nioradze,[3] H. Ohm,[1] K. Pysz,[8] R. Schleichert,[1] H. J. Stein,[1] H. Ströher,[1] K.-H Watzlawik,[1] and P. Wüstner[10]

[1]*Institut für Kernphysik, Forschungszentrum Jülich, 52425 Jülich, Germany*
[2]*Institut für Kernphysik, Universität zu Köln, 50937 Köln, Germany*
[3]*High Energy Physics Institute, Tbilisi State University, 0186 Tbilisi, Georgia*
[4]*High Energy Physics Department, Petersburg Nuclear Physics Institute, 188350 Gatchina, Russia*
[5]*Idaho Accelerator Center, Pocatello, Idaho 83209, USA*
[6]*Laboratory of Nuclear Problems, Joint Institute for Nuclear Research, 141980 Dubna, Russia*
[7]*Physikalisches Institut, Universität Bonn, 53115 Bonn, Germany*
[8]*H. Niewodniczański Institute of Nuclear Physics PAN, 31342 Kraków, Poland*
[9]*Institut für Kernphysik, Universität Münster, 48149 Münster, Germany*
[10]*Zentralinstitut für Elektronik, Forschungszentrum Jülich, 52425 Jülich, Germany*

(Received 31 March 2006; published 21 June 2006; corrected 26 June 2006)

The $pp \to pp\phi$ reaction has been studied at the Cooler Synchrotron COSY-Jülich, using the internal beam and ANKE facility. Total cross sections have been determined at three excess energies ϵ near the production threshold. The differential cross section closest to threshold at $\epsilon = 18.5$ MeV exhibits a clear S wave dominance as well as a noticeable effect due to the proton-proton final-state interaction. Taken together with data for $pp\omega$ production, a significant enhancement of the ϕ/ω ratio of a factor 8 is found compared to predictions based on the Okubo-Zweig-Iizuka rule.

DOI: 10.1103/PhysRevLett.96.242301 PACS numbers: 25.40.Ve, 13.75.Cs, 25.10.+s

Meson production near threshold has the potential to clarify important questions of hadron physics in the nonperturbative regime of quantum chromodynamics due to its comparatively simple scheme of interpretation. The production of light vector mesons, $\rho(770)$, $\omega(782)$, and $\phi(1020)$, quark antiquark states with their spins aligned ($J^P = 1^-$) and without open strangeness, has been investigated with both hadronic and electromagnetic probes in order to study production mechanisms [1], coupling constants [1], modifications in the nuclear medium [2] and, in particular, the so-called Okubo-Zweig-Iizuka (OZI) rule [3]. This rule states that processes with disconnected quark lines between initial and final states are suppressed compared to those where the incident quarks continue through to the exit channel. As a result, the production of ideally mixed ϕ mesons (quark content $s\bar{s}$) in a reaction $A + B \to \phi X$ is reduced compared to $A + B \to \omega X$ (ω is a linear combination of $u\bar{u} + d\bar{d}$) under similar kinematical conditions. Taking into account deviations from ideal mixing between singlet and octet vector mesons, Lipkin predicted a ratio of single ϕ to ω production of $R_{\phi/\omega} = 4.2 \times 10^{-3} \equiv R_{\mathrm{OZI}}$ [4,5]. However, strong enhancements of the experimental $R_{\phi/\omega}$ compared to R_{OZI} have been observed (an overview is given in Ref. [6]), in particular, in $\bar{p}p$ annihilations, where $R_{\phi/\omega}$ can be as large as $\sim 100 \times R_{\mathrm{OZI}}$ [7]. Here a strong correlation of the ϕ meson yield with the spin-triplet fraction of the initial state was found [8], and this in part motivated the suggestion of a polarized internal strangeness component in a polarized nucleon [9]. However, alternative explanations, such as two-step kaon-exchange models [10,11], have also been advanced. Since vector-meson production in close-to-threshold $pp \to ppV$ reactions must proceed via the spin-triplet entrance channel, the investigation of the cross section ratio $\sigma(pp \to pp\phi)/\sigma(pp \to pp\omega)$ at small excess energies ϵ should provide a clean way of investigating possible violations of the OZI rule.

Total cross sections for ω production in proton-proton collisions have been measured in a range of excess energy ϵ from a few MeV up to several GeV [12–14], whereas data for $pp\phi$ are very scarce. Two total cross sections of ϕ production have been obtained for $\epsilon \sim$ (2–4) GeV, but with rather limited accuracy [15,16]. At low excess energy, a single measurement of total and differential cross sections has been made by the DISTO collaboration at $\epsilon = 83$ MeV [17]. In combination with the ω cross section of COSY-TOF at $\epsilon = 92$ MeV [13], this yields $R_{\phi/\omega} \sim 7 \times R_{\mathrm{OZI}}$. The differential distributions from DISTO indicate that ϕ production at that energy proceeds dominantly via the $^3P_1$ (pp) entrance channel, though other partial waves do contribute significantly. To clarify this, it is crucial to extend the measurements to such small excess energies that only the lowest partial waves can contribute. Such measurements have become feasible at the internal proton beam of the Cooler Synchrotron COSY at the Research Center Jülich, using the ANKE target and detector facility. Here we report on the results for ϕ production in proton-proton collisions at three beam momenta, corresponding to excess energies of $\epsilon = 18.5$, 34.5, and 75.9 MeV.

ANKE is a magnetic spectrometer [18] situated at the internal beam of COSY. It comprises three dipole magnets D1–D3, which guide the circulating beam through a variable chicane. The central C-shaped spectrometer dipole D2, with a maximum field strength 1.6 T, is placed downstream of the target position. D2 is used to separate the reaction products from the circulating beam, deflecting them towards charged-particle detectors on the left (right) side of the beam for negative (positive) charges. The hydrogen cluster-jet target used provided areal densities of $\sim 5 \times 10^{14}$ cm^{-2} [19]. The average luminosity during the experiment was determined through the simultaneous measurement of pp elastic scattering. By detecting one fast forward-going proton ($\vartheta = 5.0°$–$8.5°$) in appropriate detectors, elastic events were easily separated from background. Taking the corresponding cross sections from the SAID database [20], luminosities between $(1.5–3.2) \times 10^{31}$ cm^{-2} s^{-1} were determined. The uncertainties in these contribute 4% (at $\epsilon = 18.5$ MeV), 6% (34.5 MeV), and 9% (75.9 MeV), respectively, to the final systematic error in the total cross sections.

The $pp \to pp\phi$ reaction has been studied by detecting the K^+K^- decay of ϕ mesons in coincidence with one of the forward-going protons, requiring that the missing mass be consistent with that of the nonobserved second proton. Particle identification relies on time-of-flight (TOF) measurements and the determination of particle momenta. In the initial step, positive kaons are selected by a procedure described in detail in Ref. [21], using TOF between START and STOP scintillation counters of a dedicated K^+ detection system. Second, both the coincident K^- and forward-going proton are selected from the time-of-flight differences between the STOP counters—in the negative as well as in the forward detector system—with respect to the positive STOP counter that was hit by the K^+. These two TOF selections, as well as the selection for the K^+, were done inside $\pm 3\sigma$. The absolute time calibration of all negative and forward STOP counters in conjunction with all of the positive STOP counters was performed using the abundant $\pi^+\pi^-$ and π^+p pairs. The final selection of the $pp \to ppK^+K^-$ reaction was made by a $\pm 3\sigma$ missing-mass cut on the nondetected proton. This leads to 400–1800 identified ppK^+K^- events depending on the energy. The estimated background inside the proton cut window is 5% (at $\epsilon = 18.5$ MeV), 12% (34.5 MeV), and 18% (75.9 MeV).

The left panel of Fig. 1 shows the K^+K^- invariant-mass distributions in the region around 1 GeV/c^2. For all three beam energies, a clean ϕ peak is observed at 1.02 GeV/c^2 on top of a smooth background of nonresonant kaon-pair production. The right panel shows the corresponding $pp \to pp\phi \to ppK^+K^-$ differential cross sections, i.e., distributions corrected for detector acceptances (see below). Contributions from misidentified particles have been subtracted using data from outside the proton peak in the missing-mass distributions, adding 3% (18.5 MeV), 7% (34.5 MeV), and 10% (75.9 MeV) to the final systematic error. Each spectrum has been fit with the sum of two contributions. A uniform distribution, based on four-body (ppK^+K^-) phase space, was used for the background, whereas the ϕ was modeled by its natural line shape, folded with a Gaussian function ($\sigma = 1$ MeV/c^2) to take into account the momentum resolutions of the detectors.

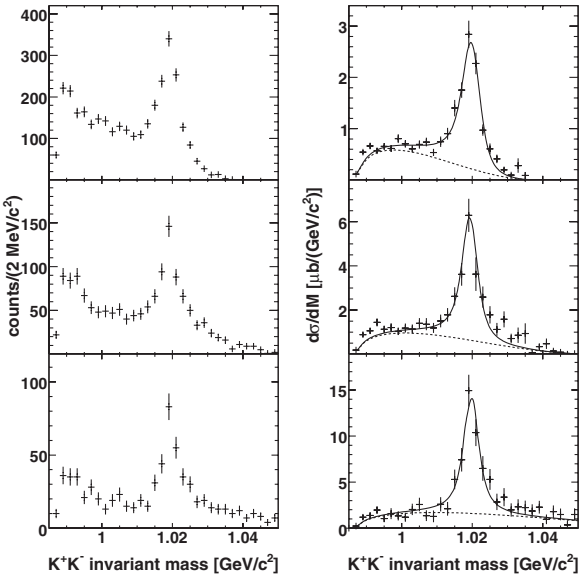

FIG. 1. K^+K^- invariant-mass distributions at $\epsilon = 18.5$ MeV (top), 34.5 MeV (middle), and 75.9 MeV (bottom). Measured raw distributions are shown on the left-hand side. while the corresponding cross sections $d\sigma/dM$ are plotted on the right. Only statistical uncertainties are shown. The cross sections contain a nonresonant part (dashed line, based on four-body phase space) and a ϕ meson contribution. The solid line is the sum of both and includes effects of the detector resolution.

Estimates of the differential acceptance of ANKE have been obtained by means of a multidimensional matrix Monte Carlo method, which allows one to determine the acceptance independent of the ejectile distributions at the production vertex (see Ref. [17]). In general, 7 degrees of freedom (dof) are needed to characterize completely the ppK^+K^- final state, but in our case, a 3D matrix has been used with the following dof: (i) the relative momentum of the two final-state protons in the (pp) reference frame, (ii) the polar angle of the K^+ meson in the rest frame of the K^+K^- system, and (iii) the K^+K^- invariant mass. Significant deviations from pure phase space can be expected close to threshold for both (i) and (ii), due to the final-state interaction between the two protons, and also the angular distribution of the decay of the ϕ mesons (see Fig. 3). The remaining dof are contained in the implicit assumption of isotropic angular distributions. These assumptions seem in retrospect to be justified since the resulting Monte Carlo simulations reproduce the measured

TABLE I. Total production cross section for $pp \to pp\phi$ at our three excess energies (Col. 1) compared to $pp \to pp\omega$ data [12,13] (Col. 2) at similar excess energies. The last column contains the ratio of ϕ to ω cross sections for each line. In all cases the first error is statistical and the second systematic.

ϕ production (ANKE)		ω production		ϕ/ω production ratio
ϵ_ϕ [MeV]	σ_ϕ(tot) [nb]	ϵ_ω [MeV]	σ_ω(tot) [μb]	$R_{\phi/\omega} \times 10^{-2}$
18.5	$43.2 \pm 2.2 \pm 5.1$	19.6 ± 0.9	$1.51 \pm 0.23 \pm 0.18$	$2.9 \pm 0.5 \pm 0.5$
34.5	$84.9 \pm 6.9 \pm 13.6$	30.0 ± 0.9	$1.77 \pm 0.48 \pm 0.23$	$4.8 \pm 1.4 \pm 0.9$
75.9	$188.0 \pm 19.1 \pm 41.4$	92	$7.5 \pm 1.9 \pm 1.5$	$2.5 \pm 0.7 \pm 0.7$

distributions within their statistical uncertainties. Each of the three variables (i)–(iii) are subdivided into 10 to 30 bins, producing in total several thousand elements, but for all of them the acceptance is nonzero. The acceptance corrections contribute 10% (18.5 MeV), 14% (34.5 MeV), and 19% (75.9 MeV) to the final systematic error.

Using the number of ϕ mesons from the fit, the integral luminosity for the measurements, and the efficiencies and acceptances of the ANKE detectors, the total ϕ meson production cross section has been deduced for the three energies, taking into account the branching ratio in ϕ decay of $\Gamma_{K^+K^-}/\Gamma_{\rm tot} = 0.491$ [5]. The results are given in Table I and plotted as a function of excess energy in Fig. 2. Very good agreement is found with the DISTO point at $\epsilon = 83$ MeV. The dashed line in the figure displays the energy dependence of phase space. When this is normalized to the highest energy ANKE point, it misses the two lower points by large factors. The solid line includes the effect of the final-state interaction (FSI) between the two protons in the $^1S_0$ state using the Jost-function method (see Ref. [22]) and scaled such that it fits best all three ANKE cross sections. The much improved agreement here means that it is crucial to include the FSI in any description of the data.

Before discussing the differential cross sections which were measured at the lowest excess energy, it is useful to note the following constraints. Close to threshold, the two final-state protons must be in the $^1S_0$ wave, and the ϕ in a relative S wave with respect to this pair, so that the initial two-proton state is the $^3P_1$. This in turn requires the alignment of the incident (pp) spin as well as of the final ϕ meson spin direction to lie along the beam axis (see Ref. [17] for a more detailed discussion). The polar angular distribution of the decay kaons in the ϕ meson rest frame must then display a $\sin^2\Theta_\phi^{K^+}$ shape relative to the beam direction, as is observed for our $\epsilon = 18.5$ MeV data in Fig. 3. Any additional $\cos^2\Theta_\phi^{K^+}$ contribution, induced by higher partial waves, is not visible. In the lower part of Fig. 3, we show from left to right the distributions in (i) the polar angle of the ϕ meson in the overall c.m. system, (ii) the polar angle of the emitted protons relative to the

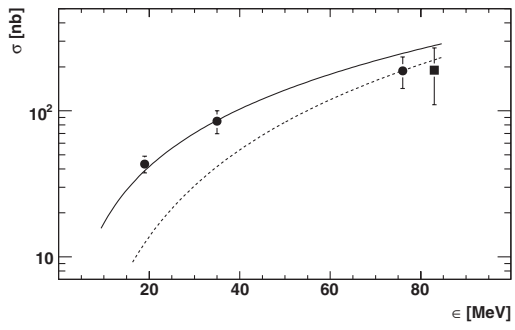

FIG. 2. Total cross section for ϕ production in pp collisions as a function of excess energy ϵ from this work (circles) and DISTO [17] (square). The error bars include both statistical and systematic uncertainties. The dashed line shows a phase-space calculation normalized to pass through the highest energy ANKE point, while the solid line, which includes pp final-state interaction effects, is a fit to all the ANKE data.

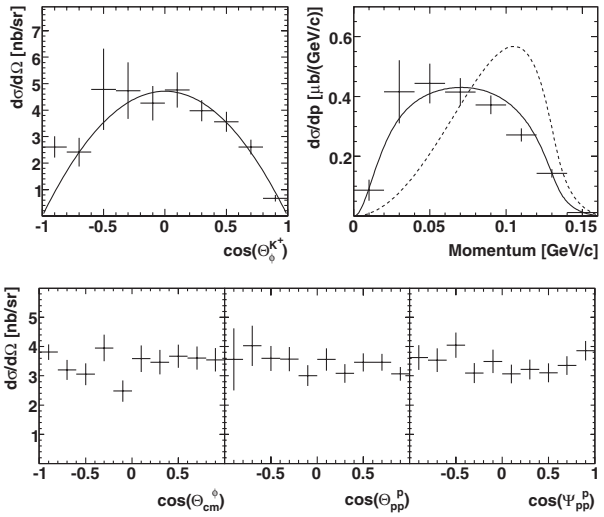

FIG. 3. Differential distributions for $\epsilon = 18.5$ MeV. Vertical error bars indicate statistical uncertainties and horizontal ones bin widths. Upper left panel: $d\sigma/d\Omega$ as a function of the cosine of the polar K^+ in the reference frame of the ϕ meson relative to the beam direction. The full line is the expected $\sin^2\Theta$ shape. Lower panels: $d\sigma/d\Omega$ vs cosine of the polar angle of the ϕ meson in the overall c.m. system (left), polar angle of the emitted proton (middle), and proton polar angle relative to the ϕ direction (right), the two latter being in the (pp) reference frame. Upper right: Dependence of the cross section on the pp relative momentum. The dotted line reflects pure phase space whereas the solid includes also the pp FSI.

beam, and (iii) the proton polar angle relative to the ϕ direction. Both proton angles are measured in the (pp) reference frame. All three distributions are consistent with isotropy, as expected for a ${}^3P_1 \rightarrow {}^1S_0$ transition. Finally, in Fig. 3 the differential cross section is plotted as a function of the proton momentum in the (pp) rest frame. While the phase-space calculation (dashed line) misses the data, inclusion of FSI for the two protons in the ${}^1S_0$ state reproduces the experimental results. Thus, a clear and significant pp final-state interaction is observed at $\epsilon = 18.5$ MeV.

While at $\epsilon = 83$ MeV DISTO also observed the dominance of the ${}^3P_1 \rightarrow {}^1S_0$ transition [17], they did not see any indication of pp FSI in their proton-momentum spectrum, and this is consistent with our findings at $\epsilon = 75.9$ MeV. Taking both results together, it is tempting to ask for the mechanism that suppresses final-state interactions at moderate excess energies: contributions of higher partial waves are an obvious conventional cause, but more exotic explanations, like a ϕN-resonance (see Ref. [22]), have also been advanced.

Turning now to the ϕ/ω ratio, we also present in Table I data on $pp \rightarrow pp\omega$ total cross sections obtained in the ϵ range of our measurement [12,13]. The last column lists the ratios as obtained line by line, i.e., at slightly different values of ϵ. Within the stated uncertainties the ratios are equal, and we have therefore calculated a weighted mean by first fitting and interpolating the ω results to our excess energies. This gives

$$R_{\phi/\omega} = (3.3 \pm 0.6) \times 10^{-2} \sim 8 \times R_{\mathrm{OZI}},$$

as compared to an uncorrected weighted mean of the last column of Table I, which is about 10% smaller. Taking into account the effects of the finite meson widths on the phase space [12,22] changes R_{OZI} by at most 5% at the lowest excess energies.

The production ratio obtained from high energy ppV data is $\sim(1\text{–}2.4) \times R_{\mathrm{OZI}}$ [14–16]. Together with our findings, this means that there must be a significant energy dependence of the OZI enhancement factor [22], which requires more theoretical work to understand its origin. In this context let us mention that the experimental ratio $R_{\phi/\omega}$ deduced from πN interaction gives $(3.2 \pm 0.8) \times R_{\mathrm{OZI}}$ [23], which can be explained in terms of the established OZI violation in the $\phi\rho\pi$ and $\omega\rho\pi$ coupling [5,24]. The present ratio from near-threshold ϕ and ω production in pp collisions exceeds this value by more than a factor of 2. It may be a signal for additional, and as yet nonunderstood, dynamical effects related to the role of strangeness in few-nucleon systems.

In summary, we have measured cross sections for ϕ production in pp interactions at three excess energies, all of which are much closer to threshold than previous data. The lowest energy result demonstrates the dominance of the transition from the ${}^3P_1$ (pp)-entrance channel to the ${}^1S_0$ (pp) final state. Both the total cross section and the proton-momentum spectrum indicate a significant pp final-state interaction. Using data for ω production from literature, it is found that $R_{\phi/\omega}$ is about $8 \times R_{\mathrm{OZI}}$.

Useful discussions with J. Haidenbauer, C. Hanhart, U.-G. Meißner, A. Sibirtsev, C. Wilkin and members of the ANKE Collaboration are gratefully acknowledged. Our thanks apply also to the COSY machine crew for their support. This work was supported by: BMBF, DFG, Russian Academy of Sciences, and COSY FFE.

*Electronic address: M.Hartmann@FZ-Juelich.de

[1] K. Tsushima and K. Nakayama, Phys. Rev. C **68**, 034612 (2003); A. Faessler *et al.*, Phys. Rev. C **70**, 035211 (2004); L. P. Kaptari and B. Kämpfer, Eur. Phys. J. A **23**, 291 (2005).
[2] M. Naruki *et al.*, Phys. Rev. Lett. **96**, 092301 (2006).
[3] S. Okubo, Phys. Lett. **5**, 165 (1963); G. Zweig, CERN Report No. TH-401, 1964; J. Iizuka, Prog. Theor. Phys. Suppl. **37–38**, 21 (1966).
[4] H. J. Lipkin, Phys. Lett. B **60**, 371 (1976); current data lead to $R_{\mathrm{OZI}} = 3.53 \times 10^{-3}$, see Ref. [5].
[5] S. Eidelmann *et al.*, Phys. Lett. B **592**, 1 (2004).
[6] V. P. Nomokonov and M. G. Sapozhnikov, Phys. Part. Nucl. **34**, 94 (2003).
[7] C. Amsler *et al.*, Rev. Mod. Phys. **70**, 1293 (1998).
[8] A. M. Bertin *et al.*, Phys. Lett. B **388**, 450 (1996).
[9] J. Ellis *et al.*, Phys. Lett. B **353**, 319 (1995); Nucl. Phys. **A673**, 256 (2000).
[10] U.-G. Meißner *et al.*, Phys. Lett. B **408**, 381 (1997).
[11] M. P. Locher and Yang Lu, Z. Phys. A **351**, 83 (1995).
[12] F. Hibou *et al.*, Phys. Rev. Lett. **83**, 492 (1999).
[13] S. Abd El-Samad *et al.*, Phys. Lett. B **522**, 16 (2001).
[14] A. Baldini *et al.*, in *Numerical Data and Functional Relationships in Science and Technology, Total Cross Sections for Reactions of High Energy Particles*, edited by H. Schopper, Landolt-Börnstein, New Series, Group 1, Vol. 12 (Springer-Verlag, Berlin, 1998).
[15] R. Baldi *et al.*, Phys. Lett. B **68**, 381 (1977).
[16] V. Blobel *et al.*, Phys. Lett. B **59**, 88 (1975).
[17] F. Balestra *et al.*, Phys. Rev. C **63**, 024004 (2001).
[18] S. Barsov *et al.*, Nucl. Instrum. Methods Phys. Res., Sect. A **462**, 364 (2001).
[19] A. Khoukaz *et al.*, Eur. Phys. J. D **5**, 275 (1999).
[20] R. A. Arndt *et al.*, Phys. Rev. C **62**, 034005 (2000); http://gwdac.phys.gwu.edu, SAID solution **SP04**.
[21] M. Büscher *et al.*, Nucl. Instrum. Methods Phys. Res., Sect. A **481**, 378 (2002).
[22] A. Sibirtsev, J. Haidenbauer, and U.-G. Meißner, Eur. Phys. J. A (to be published).
[23] A. Sibirtsev and W. Cassing, Eur. Phys. J. A **7**, 407 (2000).
[24] M. Gell-Mann and F. Zachariasien, Phys. Rev. **124**, 953 (1961); U.-G. Meißner, Phys. Rep. **161**, 213 (1988).